Evaluation of Low Molecular Weight Cross Linked Chitosan Nanoparticles, to Enhance the Bioavailability of 5-Flourouracil

Aisha Sethi[1,2] ⓘ, Mahmood Ahmad[1], Tayyaba Huma[3], Ikrima Khalid[2], and Imtiaz Ahmad[1]

Abstract

The present study aimed to formulate 5-fluorouracil loaded cross linked chitosan nanoparticles based on chemical cross-linking of low molecular weight chitosan with glutaraldehyde by reverse micelles technique as 5-FU is less hydrophobic, relatively potent, has a shorter half-life, is rapidly metabolized, less tolerated, and has low oral bioavailability; therefore, we aimed to formulate potential nanocarriers of 5-FU for efficient drug delivery to specific targeted areas of action, reduce oral toxicity, improve tolerability and therapeutic outcomes of 5-FU, in a restricted fashion to enhance the bioavailability of 5-FU. Nanoparticles were formulated by the reverse micelle method based on the chemical cross-linking of glutaraldehyde (25% aqueous solution) into a w/o emulsion in different ratios. LMWCH-NPs were characterized for post-formulation parameters by mean particle size, zeta potential, %age yield, loading/entrapment efficiency, Fourier transform infrared spectroscopy (FTIR), DSC/TGA, TEM, PXRD, drug release at pH 1.2, and pH 7.4. 5-FU loaded NPs showed a size range (198 nm-200 nm) and zeta potential (-39mV to -41mV), which ensured mechanical stability and increased retention time in blood vessels by the sustained release properties of biodegradable nanocarrier drug delivery systems. % age yield showed the range 92% to 96% while % LC ranged 2.0% to 3.4% and %EE ranged 40% to 43%. The TEM images showed spherical nanoparticles. FTIR revealed the compatibility between the drug and the cross-linked polymer. DSC/TGA ensured the thermal stability of the drug, while the solid-state stability of the drug-loaded cross-linked chitosan nanoparticles was evaluated by powder X-ray diffraction (PXRD) analysis. Drug release studies were performed using the dialysis bag technique at both pH (1.2 and 7.4) to mimic the gastrointestinal tract. Highly stable NPs displayed targeted release in phosphate buffer pH 7.4 at 37°C. Fickian diffusion was the predominant release with an R^2 value of 0.9975-0.9973—and an N value 0.45-0.53. Prepared nanoparticles are inert, biodegradable, and biocompatible drug delivery systems for sustained release of 5-FU with maximum therapeutic efficacy and bioavailability.

Keywords

5-flourouracil, cross linked, nanoparticles, chitosan, bioavailability

Introduction

Uncontrolled growth and proliferation of cells is called cancer, which results in tumor formation, and these tumors can be cancerous (malignant) or non-cancerous (benign). Global Cancer Statistics in 2020 reported about 10 million deaths while it was found to be elevated up to 18.1 million new cases of cancer,[1] while inconsequential endurance rate, nonspecific cytotoxicity of malignant cells, *in vitro* progression of multi-drug confrontation toxicity were the conventional unresolved problems.[2] Such side effects of conventional chemotherapeutic agents alone, either in combination, indicate that more efforts were focused instantly to improve efficacy, which badly

[1] Faculty of Pharmacy and Alternative Medicines, The Islamia University of Bahawalpur, Punjab, Pakistan
[2] Faculty of Pharmaceutical Sciences, Government College University, Faisalabad, Punjab, Pakistan
[3] Akhuwat First, Faisalabad, Punjab, Pakistan

Corresponding Author:
Mahmood Ahmad, Faculty of Pharmacy and Alternative Medicines, the Islamia University of Bahawalpur 63100, Punjab, Pakistan.
Email: ma786_786@yahoo.com

affected socioeconomically. Although different anticancer agents are available for the treatment of various types of cancers, insufficient drug release due to unspecified targeted site of action can harm other body tissues. A passive targeted drug delivery system facilitates chemotherapeutic agents at targeted areas of action without any ligand (active targeting).[3] Leaky vasculatures on the surface of cancerous cells, which allows NPs to improve vascular permeability and prolong the residence time of the drug carrier at the site of action (cancerous cells). This requirement could be made possible by a nanocarrier drug delivery system, with efficient and targeted drug delivery systems[3] and named the enhanced permeability and retention (EPR) effect.[4-7]

Modern researchers have synthesized NPs with added benefits, that is, stable and compact behavior in response to the external environment, termed smart, intelligent, or environmentally sensitive or responsive nanoparticles.[8] Drug-delivery systems (DDSs) based on nanotechnology are novel approaches for the pharmaceutical industry. Nanotechnology comprises nanoscale in 3 dimensions, called nanoparticles (NPs). The major goals in designing nanoparticles as an oral drug delivery system (ODDSs) were found to improve solubility, dissolution rate, control drug release rate, and target specificity of drug(s), ultimately enhancing their bioavailability.[9] These nanosized drug carriers are prepared using polymeric nanoparticles with hydrophilic, hydrophobic, biodegradable, biocompatible, and non-toxic polymers using different nanoparticles formulation techniques embedded in physical and chemical methods, including primary and multiple emulsion solvent evaporation methods, ionic gelation, spray-drying, supercritical fluid technology, and precipitation with a compressed fluid technique anti-solvent. Chemical synthesis of silica nanoparticles with patchy internal structures has been used to modify the solubility, permeability, and bioavailability of therapeutic agent(s).[10]

Chitosan is a biopolymer, biocompatible, nontoxic amino polysaccharide (poly-1,4-D-glucosamine) of natural origin, obtained by the deacetylation of chitin. It is derived from crustacean shells, insect cuticles and cell walls of fungi, and is widely used as a stabilizing or suspending agent for different oral drug delivery systems, as chelating agents for the removal of toxic metals, nuclear wastes and in ion exchange processing of many other industries, while chitosan-NPs undergo various external factors that stimulate rapid diffusion of drugs throughout the meshwork.[8] In a recent study, we showed that drug diffusion from a chitosan network could be efficiently controlled or restricted by a cross-linking matrix using a dialdehyde such as glutaraldehyde[11]

5-Fluorouracil (5-FU), an anticancer drug introduced in 1958, has higher therapeutic efficacy in solid tumors, such as colon, rectum, and breast cancers. Its oral conventional brand shows erratic absorption through the GIT. As it shows rapid gastrointestinal absorption, after oral administration, it yields peak blood levels between 15 and 60 minutes.[11] Additionally, 5-FU has nonspecific toxicity in normal healthy cells, rapid renal clearance, and metabolism by dihydropyrimidine dehydrogenase (DPD) enzyme, and high digestive distress inhibits its application in the management of cancer. It has been reported that 80% of orally administered 5-FU metabolizes the liver and kidney.[12,13] It has been detoxified and excreted as F-ß-alanine by urine. However, due to the high rate of metabolism in blood, it also has a shorter half-life (8-20 min).[14] Intravenous administration of 5-FU for solid types of cancers demonstrates severe cytotoxic effects in a large number of previous studies. As intravenous administration of 5-FU was disturbed microbial flora of GIT track so, accurately designed oral formulations of 5-FU using different biocompatible, biodegradable, smart pH sensitive polysaccharides have employed for sustained, controlled delivery of therapeutic agent i.e. depending upon selection of polymer and networking pattern on tumor cells by most of researchers in the literature as well. Cross-linking can also influence drug loading and entrapment efficiency from NPs, which affect therapeutic diffusion and tunable physiochemical properties of nanocarriers or nanoparticles, facilitating sustained or controlled release of the drug at the targeted site of the tumor without harming the other body tissues.[15,16]

Therefore, the major focus of our study was to develop and evaluate low-molecular-weight cross-linked chitosan nanoparticles as novel drug delivery carriers that may offer enhanced efficiency and reduce toxicity by improving dissolution, solubility, bioavailability of 5-Fluorouracil (5-FU) for the treatment of various solid types of cancers.

Materials and Methods

5-Fluorouracil powder was a kind gift from Pharmedic Laboratories (Pvt.) Ltd. Lahore, Pakistan. LMWCH (50,000-190,000 Da), glutaraldehyde (25% aqueous solution), and sorbitan monooleate (Span 80) were purchased from Sigma-Aldrich (UK). Dialysis bags (molecular weight cut-off value 8000 Da) were purchased from Spectrum Labs (Germany). Miglyol oil of medicinal grade, acetic acid (99.9% purity), potassium dihydrogen phosphate, and sodium hydroxide were purchased from Merck (Germany). All other ingredients were of analytical grade and were purchased from a local chemical vendor.

Formulation of 5-FU/GA-co-LMWCH-NPs

Glutaraldehyde (GA), based on cross-linked low-molecular-weight chitosan nanoparticles, was prepared using the reverse micellar method as described[17,18] in Figure 1. For the aqueous phase, different amounts of chitosan (LMWCH) were weighed and dissolved in 1% v/v acetic acid. An aqueous solution of the drug was prepared at approximately 5 mg per 100 mg of polymer solution, which was mixed and heated for 2 to 4 min at 60°C. For the oil phase, the primary emulsion w/o was prepared using 2 ml of Migylol oil as the external/continuous phase in a 10 ml glass vial using a high-speed homogenizer. Span 80 was used as a surfactant at various concentrations. Both aqueous and oil phase dispersions were stirred with a magnetic stirrer of 1 cm at different speeds for 2-5 h to obtain a stable emulsion.
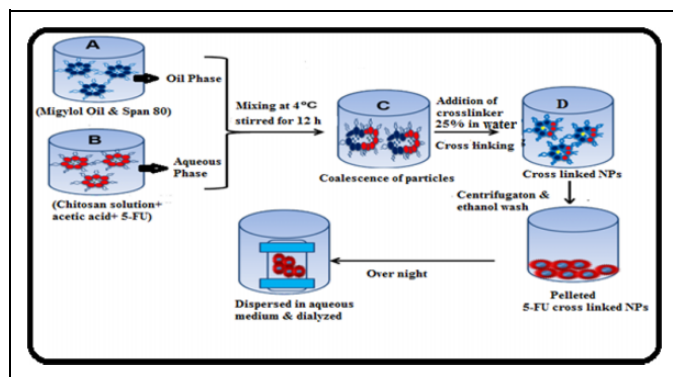
Figure 1. Schematic preparation of 5-FU/GA-LMWCH-NPs.

After homogenization, a stable emulsion was formed and the pH of the solution was adjusted from 4 to 5, and various concentrations of cross-linker glutaraldehyde (GA) were added at different time intervals. This dispersion was stirred at a constant stirring speed of 900 rpm at 45°C for at least 5 h or left overnight using a magnetic stirrer. This dispersion was then subjected to centrifugation at 14000 rpm at 4°C for 15-30 min. The supernatant solution was decanted, which contained drug-loaded low-molecular-weight chitosan NPs, and pellets were suspended in ethanol to wash off the oil phase. The washing/centrifugation steps were repeated 2-3 times, followed by washing twice with methanol and then once with distilled water. Finally, the NP pellets were collected by filtration and lyophilized for further physicochemical characterization.

Particle size, Polydispersity Index (PDI) and Zeta Potential (mV)

The particle size of NPs was used to determine the therapeutic efficiency at the targeted site of action (passive targeting), while the polydispersity index (PDI) and zeta potential determined colloidal homogeneity and stability. Particle size, PDI, and zeta potential were measured using a Malvern Nano ZS 90 Zetasizer instrument (UK) at 25°C.[19,20]

Percentage Yield of NPs

It was measured by an indirect method and the percentage yield of the prepared NPs was calculated by the percent product yield of 5-Fluorouracil loaded chitosan NPs to determine the efficiency and suitability of the preparation method.[21,22]

% yield of NPs was calculated by following formula:

$$\% \text{ yield} = \frac{\text{Mass of nanoparticles obtained}}{\text{Total mass of all excipients} + \text{drug}} \times 100$$

Drug Loading Capacity (%LC) and Entrapment Efficiency (%EE)

Drug loading (%LC) and entrapment efficiency (%EE) were calculated using an indirect method. In this method, the

prepared 5-FU loaded NP formulations were subjected to centrifugation at 15,000 rpm for 15 min to settle down the NP fragments and quantify the amount of unentrapped drug[22,23] in the supernatant using a standard calibration curve of 5-FU via ultraviolet spectroscopy at a wavelength of 260 nm. To minimize handling errors, the analysis was performed in triplicate. This was estimated using the following formula:

$$\text{LC } (\%) = \frac{\begin{array}{c}\text{Total amount of drug in NPs} \\ - \text{ amount of unentrapped drug}\end{array}}{\text{Total weight of total NPs}} \times 100$$

$$\text{EE } \% = \frac{\begin{array}{c}\text{Total amount of encapsulated drug in NPs} \\ - \text{ amount of unentrapped drug}\end{array}}{\text{Total weight of drug in NPs}} \times 100$$

Transmission Electron Microscopy (TEM)

Transmission electron microscopy (TEM, TEM-JSM-7500F; JEOL, Tokyo, Japan) was used to determine the morphology of the NPs. A small drop of aqueous dispersed NPs with the addition of 10 μL of 1% phosphotungstic acid was drop-cast onto a carbon-coated copper grid. This was followed by air drying of the wet grid under strict sink conditions. The grid was loaded on top of the sample holder and inserted into the TEM, and photographs of the sample were recorded at a suitable voltage and different magnifications power at 10 keV.[21,24]

FTIR Spectroscopy (Fourier Transform Infra-Red Spectroscopy)

FTIR is an analytical technique that was used to evaluate the interaction and compatibility via identification of functional groups present in NP formulation components that determine the stability of the prepared and optimized nanoparticle formulations. FTIR vibrational frequency peak analysis assembly was performed using a Thermo Nicolet spectrometer (Tensor 27 series, Germany), using the KBr pellet method in the range of 4000-400 cm^{-1}. Empty cells were scanned and taken before sample analysis after locking the pressure arm by placing a small amount of sample on the crystal surface KBr disc.[23]

DSC (Differential Scanning Calorimetry)

Thermal analysis of NPs was performed by DSC analysis to determine the phase transition in the sample as a function of time and temperature in a controlled fashion through a graph between temperature (°C) and flow of heat in (w/g), using a TA instrument USA model Q600 series. After loading up to 450°C, the furnace was heated from ambient temperature of 15°C/min °C /min in a nitrogen atmosphere with a flow rate of 10 mL.min^{-1}.[23]

TGA (Thermo Gravimetric Analysis)

Thermogravimetric analysis (TGA) was used to demonstrate the percent weight loss by elevating temperature through the graph between temperature (°C) and percent weight loss using a TA Instruments Q600 series Thermal Analysis System (TA Instruments, West Sussex, UK). Five milligrams of sample was weighed and placed in an open pan (platinum 100 μL) attached to a microbalance. The samples were heated at 20 °C.min^{-1} from to 25-500 °C under dry nitrogen in standard mode with a ramp test type. Sampling was performed in triplicate.[23]

Powder X. Ray Diffraction Studies (PXRD)

X-ray diffractograms using a PXRD diffractometer (Bruker D8 Advance, Germany) using Ni-filtered Cu K ά radiation with scanning speed of 0.05°.min^{-1} having 45 KV source tube voltage, 40 mA electric current and over 10°-60° range of diffraction angle(2θ) range.[25]

Drug Release Studies by UV-Vis Spectrophotometer

The drug release behavior of all NP formulations was determined by dissolution studies, which were used as a substitute for *in vivo* drug release studies. In this study, a dialysis membrane was used with a USP dissolution apparatus type II with a paddle assembly (Pharma Test, Germany). A cellulose ester dialysis bag (molecular weight cut-off value of 10,000 Da) was chosen based on the molecular weight of the drug as well as the size of the NPs. The NPs equivalent to 5 mg of 5-FU were placed in a dialysis bag and tied at both ends with thread or clips. The filled dialysis bags were placed in a dissolution apparatus containing 250 ml dissolution medium, that is, phosphate buffered saline (PBS) at pH 7.4. Dissolution studies were carried out by adjusting the speed of the paddle at 50 rpm, while the temperature of the medium was maintained at 37°C $\pm$ 2 to evaluate the pH and thermoresponsive acidic hydrophilic drug release studies.[26,27] The samples were taken out at predetermined time intervals and their absorbance was measured using a UV-Vis spectrophotometer (IRMECO, U2020, Germany) at λmax 260 nm after 10 dilutions. Absorbance was fitted to the straight-line equation of the calibration curve to calculate the amount of 5-FU released from the prepared NPs, as shown in Figure 2.

Dissolution Kinetics Studies

The drug release mechanism from NPs was evaluated using a model-dependent approach recommended by the FDA for comparison of drug release. Model-dependent drug release data were analyzed using various kinetic models: zero-order, first-order, Higuchi, Hixson Crowell, and Korsmeyer-Peppas with DDSolver, an extension of MS. Excel.[27]
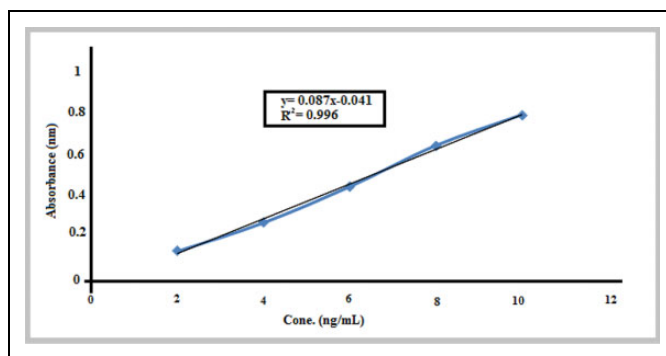

Figure 2. Standard curve of 5-fluorouracil.

Table 1. Result of Size (nm), PDI and Zeta Potential (mV) of 5-FU/GA-co-LMWCH-NPs.

Formulation code	Average particle size (nm)	Zeta potential (mV)	PDI
5FU1	198	−39	0.2
5FU2	198.1	−34	0.1
5FU3	198.7	−25.5	0.1
5FU4	198.9	−35	0.2
5FU5	198.9	−39.5	0.1
5FU6	200	−41	0.2

Physical Stability Studies

NPs (5 mg/ml), it was noted that EE% of 5-FU LMWCH-NPs stored at, 25 °C, 45 °C and 4 °C were the most stable formulations in terms of drug retention as the data indicated an insignificant change ($P > 0.05$) in the EE% of all formulations (F2, F3, and F6).[20]

Statistical Analysis

It was applied to %age yield, %EE, %LC, and particle size and zeta potential studies. Significant or non-significant data interpretation at 95% confidence interval was compared with a statistical one-tailed t-test; $P < 0.05$, was considered statistically significant difference in results.

Results and Discussions

Particle Size of NPs

The diameter of the prepared low-molecular-weight cross-linked chitosan NPs containing 5-FU was analyzed using dynamic light scattering. The average particle size for all NP formulations 5FU1 to 5-FU6 was 198-200 nm and the mean hydrodynamic diameter of particles, that is, 5-FU3, was 198.7 nm, as determined in Table 1 and Figure 3A. 5-FU3 showed a decreased zeta potential (mV) of −25.5 mV, a low polydispersity index (PDI) value of 0.1, in the water phase and showed high colloidal stability due to the cross-linking agent glutaraldehyde (GA). Size-controllable micelle-based NPs
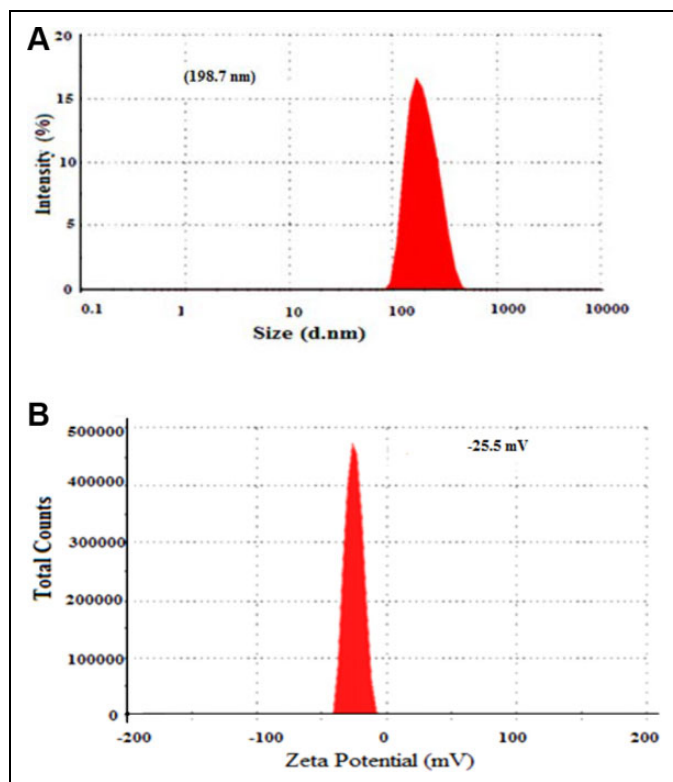
Figure 3. A, Size distributions by intensity, zeta size (5-FU3). B, Size distributions by intensity, zeta potential (5-FU3).

Table 2. % Yields of NPs Prepared From Different Formulations of 5-FU/GA-co-LMWCH-NPs.

NPs formulations	% Yield
5FU1	92.63
5FU2	85.4
5FU3	96.5
5FU4	96.5
5FU5	95
5FU6	96

offer real-time improved therapeutic efficacy and ultimately enhance the bioavailability of loaded 5-flourouracil. Lia et al have shown that nanosuspension, as well as PDI less than 0.1, increased the stability of nanocarrier therapeutic agents for liver targeting.[18,28]

Zeta Potential Analysis

This was used to characterize the surface charge of the drug-loaded LMWCH-NPs. Reducing agglomeration and enhanced colloidal stability resulted in increased electrostatic repulsion between particles at the level of a high magnitude of zeta potential for all NP formulations from 5-FU1 to 5-FU6, as illustrated in Table 2. Because particle stability mainly depends on the electrical charge of the surface, properties such as cellular uptake, rate of drug release, and blood retention time are

Table 3. LC (%) and EE (%) of 5-FU/GA-co-LMWCH-NPs.

NPs formulations	LC (%)	EE (%)
5FU1	2.0	42.1
5FU2	2.10	41
5FU3	2.0	43
5FU4	2.1	40.1
5FU5	2.0	40
5FU6	3.4	42.1

directly correlated with the zeta potential value. There was a direct association between the zeta potential (mV) of low-molecular-weight cross-linked chitosan NPs and the volume of surfactant used in the oil phase. The zeta potential of 5-FU/GA-LMWCH-NPs was found to be -25.5 mV to -41 mV, as shown in Figure 3B. This value was confirmed by subsequent nanoparticle formulation, as previously reported, and the zeta potential of LMWCH-5FU-NPs was -26.9 mV to -41 mV, which was confirmed by TEM analysis.[20]

Product Yield of NPs

The synthesized nanoparticle formulations from 5-FU1 to 5FU6 were found to yield 92.63% to 96% with more than 85% yield, but it was decreased due to unstable emulsion or due to phase separation. Moreover, these emulsion droplets were removed during the washing of NPs, leading to a low yield, as shown in Table 2, and the optimized NP formulations 5-FU3 and 5-FU4 showed 96.5% yield of all formulations. In accordance with previously reported results, 5-FU NPs yield 100% due to more compact and stable cross-linked NPs.[22]

Drug Loading and Entrapment Efficiency (LC% & EE %)

LC% and EE% of 5-FU loaded LMWCH-NPs were measured by an indirect method, as it showed a positive correlation between LC% and EE%, as shown in Table 3 for 5FU1-5FU6, LC % 2.0. 3.4%, and EE% 40%-43%, respectively. Formulation 5FU3 showed LC % 2.0, with a greater entrapment efficiency of 43%, while 5-FU6 showed greater LC % with less EE (42.1%), which might be due to the lower number of stable cross-links caused by loose binding with the cross-linker glutaraldehyde. Our results are in accordance with a previous report that hydrophilic and low lipid solubility of 5-FU, both LC% and EE% were relatively decreased, while EE% decreased sharply due to the greater volume of cross-linking agent but decreased stability or porosity of the NP polymeric network.[24]

Transmission Electron Microscope (TEM)

The internal structure of the 5-Loaded low molecular weight cross linked chitosan NPs (5-FU-LMWCH-co-NPs) was observed using transmission electron microscopy (TEM). TEM image of 5-FU loaded LMWCH-NPs was revealed in Figure 4,

somewhat curved shape but on the whole were sphere-shaped NPs. The TEM images are smaller than the hydrodynamic diameter, which might be due to the inappropriate cross-
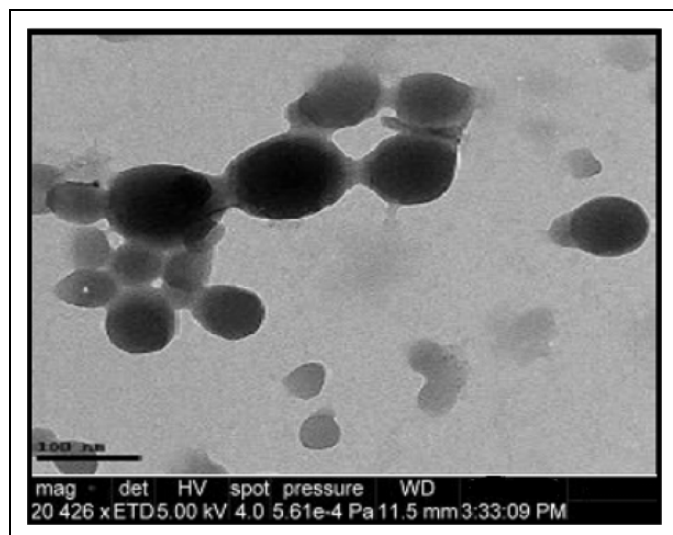

Figure 4. TEM micrograph of 5-FU/GA-co-LMWCH-NPs.

linking of glutaraldehyde (GA) during freeze-drying. Our optimized formulation, 5-FU3, showed TEM analysis of nanosized particles with a porous surface due to the penetration of surrounding water molecules. These results were previously reported for the rapid removal of 5-FU from 5-FU loaded CH-NPs due to proper cross-linking of nanosized particles with proper dispersion of the drug.[29]

Fourier Transformed Infrared Spectroscopy (FTIR)

FTIR spectra of pure polymer (LMWCH), 5-FU, physical mixture (PM), unloaded LMWCH-NPs, and loaded 5-FU-LMWCH-NPs were obtained to determine the compatibility between drug and polymer reactions to ensure NP formulation. FTIR spectra of pure LMWCH shown in Figure 5A, a wide band peak showed attached $-OH$ at 3355.42 cm^{-1} & symmetrical stretching vibration of amine N-H at 2875.28 cm^{-1}, respectively. A characteristic peak at 2875 cm^{1} corresponds to the $-CH_2$ group stretching vibration correlated to pyranose ring,[30] and a stretching vibration peak at 1374.80 cm^{-1} was observed -CH$_3$ in the amide group.[31] The characteristic band peaks of the -C-O stretching vibration at 1028.62 cm^{-1} and 1149.95 cm^{-1}, respectively. The peak at 1653.30 cm^{-1}
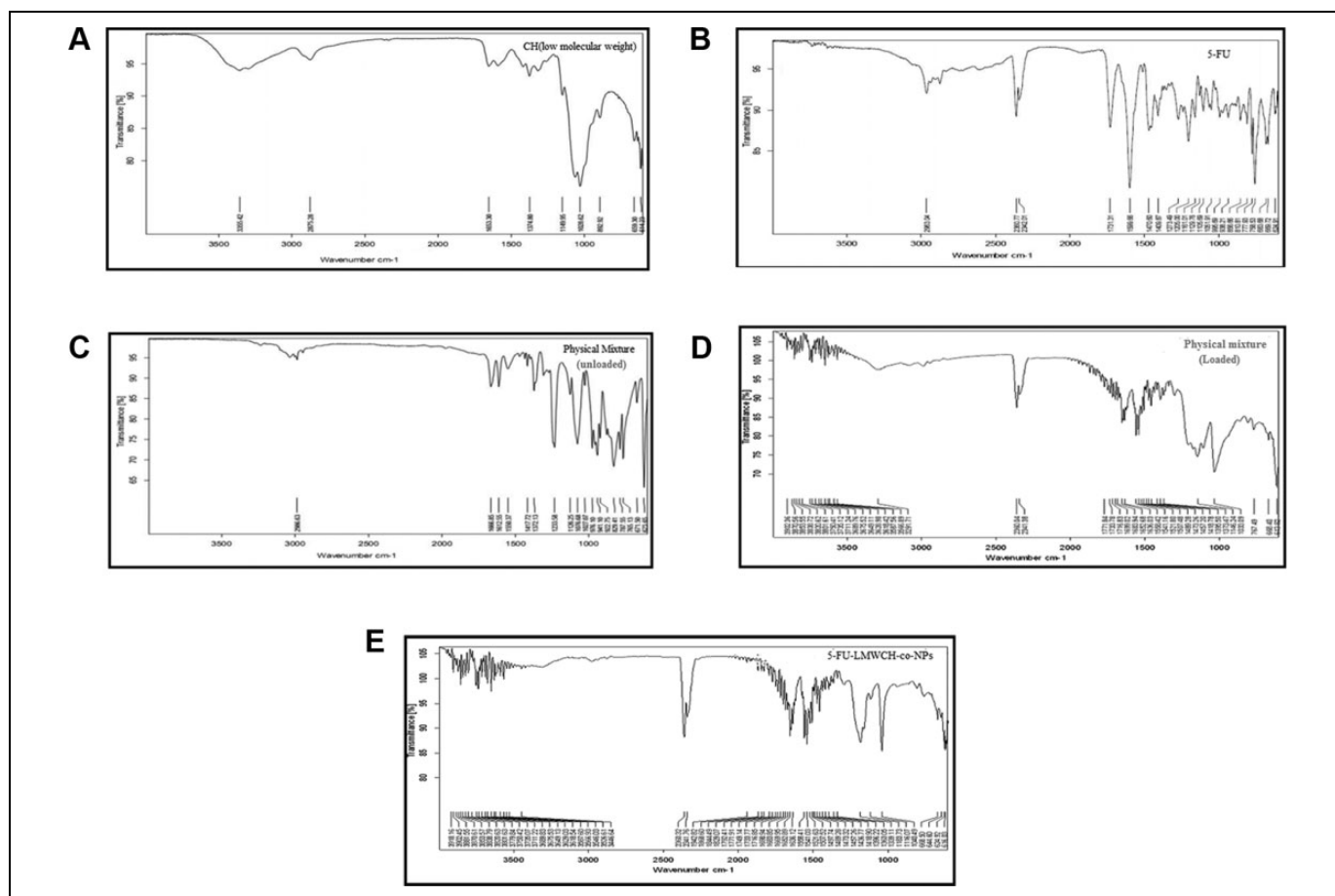

Figure 5. A, FTIR Spectrum of low molecular weight Chitosan (LMW CH). B, FTIR Spectrum of 5-FU. C, Physical mixture FTIR Spectrum of unloaded LMWCH-co-GA-NPs. D, Physical mixture FTIR spectrum of 5-FU/GA-co-LMWCH-NPs. E, FTIR Spectrum of 5-FU/GA-co-LMWCH-NPs.

corresponds to -C = O stretching of the amide group.[9] The FTIR spectra of the pure drug (5-FU) shown in Figure 5B, various characteristic band peaks, mimicking the N-H stretching vibrations of alkanes, showed peaks between and 3100-3500 cm^{-1}. A broad band spectral peak of N-H stretching vibrations[31] was observed at 3110 cm^{-1} and 3066 cm^{-1}, which can be assigned to C-H stretching vibrations, and the peaks at 2930 cm^{-1} and 2828 cm^{-1} can be attributed to –CH2– asymmetric and symmetric vibrations. FTIR analysis of 5-FU was performed at 1720 cm^{-1} for C = O stretching, C-N stretching at 1644 cm^{-1}, C-H in-plane stretching at 1242 cm^{-1}, C-F stretching at 1222 cm^{-1}, N–H and C–H wagging vibration at 994 cm^{-1}, and pyrimidine ring vibration[32] at 748 cm^{-1}. The FTIR spectral peaks of the physical mixture of unloaded LMWCH-NPs, as shown in Figure 5C, and the general characteristic peaks at 1700-1600 cm^{-1} correspond to the absorption bands of the amide I group, and 1500-1550 cm^{-1} of the N-H bending group and at 2800-2900 cm^{-1} C-N stretching, respectively. FTIR spectral peaks of physical mixture of loaded LMWCH-NPs that has been mentioned in Figure 5D, corresponds to alcoholic O-H stretching at 3292.74 cm^{-1}, methyl and C-H stretching vibration group at 2927.62 cm^{-1} C-O ether stretching vibration[28] at 1021.63 cm^{-1}. The FTIR spectra of 5-FU loaded low molecular weight chitosan NPs are also shown in Figure 5E. 5-FU loaded LMWCH-NPs, peaks between 3300 and 3400 cm^{-1} primary amine ($-$ NH), stretching of 5-Flouorouracil was present, which revealed that 5-FU presented as an intact to low molecular weight chitosan nanoparticles (5-FU loaded LMWCH-NPs), without chemical modification, as reported in the literature.[22,33]

Powder X-Ray Diffraction Analysis (PXRD)

Powder X-ray diffraction was used to study the crystalline or amorphous nature of pure low-molecular-weight chitosan, cross linker (GA), LMWCH-NPs, 5-FU, and loaded LMWCH-NPs. PXRD of pure LMWCH showed the distinct and intense peak in the range of 2θ of 20° which represented its crystalline nature with insignificant amorphous ingredients[34] as it shown in Figure 6A. The PXRD diffraction pattern of the cross-linking agent glutaraldehyde (GA 25% aqueous solution) displayed no intense characteristic peaks; only a hump peak pattern was observed,[35] as illustrated in Figure 6B. The PXRD diffraction pattern of the pure polymer of low molecular weight chitosan (MMWCH-NPs) showed moderately sharp diffraction[36] at 2θ = 12.5°, 15.2°, 18.5°, 20.1°, 23.5°, and 31.5°, and less diffraction at 2θ = 22.5°, 34.6°, 35.8°, and 39.5°, respectively, as shown in Figure 6C. The PXRD profile of low-molecular-weight chitosan-NPs (LMWCH-co-GA-NPs) showed a reduction in crystalline structural characteristics compared to pure low-molecular-weight chitosan nanoparticles (GA-co-LMWCH-NPs). Generally, most polymers may have an amorphous or semi-crystalline structure. The crystallinity may be due to the integration of new bulkier groups within low-molecular-weight chitosan nanoparticles (GA-co-LMWCH-NPs) via chemical crosslinking of glutaraldehyde, which was previously reported as an intense sharp peak at 2θ = 15.6°,

16.2°, 18.6°, 20.6°, 28.4°, and 32.1° by Ziyaur et al (2005). The PXRD diffractogram of 5-Fluorouracil showed a sharp single peak and the highest peak at $2\theta = 16.1$°, which indicates the crystalline nature of 5-FU, while some moderately intense peaks at 15.1°, 19.5°, 24.06°, 30.35°, and 35.49° at 2θ scale,[37] corresponding to the crystalline nature of 5-Fluorouracil, as shown in Figure 6D. 5-FU PXRD analysis showed peaks at 2θ = 15.9°, 16.2°, 18.9°, 20.6°, 28.5° and 32.1° indicating strong and sharp. 5-FU showed an intense sharp peak at $2\theta = 28.0$°, when entrapped with low-molecular-weight chitosan, the peak departed.[38] XRD analysis of 5-FU loaded LMWCH-NPs showed different peak fashion than the XRD pattern of pure components due to differences in their crystalline and non-crystalline functions, which were determined by XRD). 5-FU/GA-co-LMWCH-NPs with decreased crystalline or amorphous nature show the distribution of 5-FU at the molecular level encapsulated in the matrix or network of nanoparticles, as shown in Figure 6E. Therefore, the degree of crystallinity of the polymer and the cross-linking process can be explained by PXRD analysis.[37]

Thermal Analysis (DSC-TGA)

The thermal properties of both qualitative and quantitative information about the physicochemical state of the drug within the NPs were studied using DSC-TGA thermograms. When the drug was loaded inside the NPs as a solid dispersion, there was no visible endotherm peak, as shown in Figure 7A and the DSC thermogram of low molecular weight chitosan NPs (LMWCH-co-NPs) initially showed a slight endothermic peak at 90°C while a sharp endothermic peak at 220.79°C[39] was observed, indicating of degradation in temperature at the same time breakdown of the amine group of low-molecular-weight chitosan nanoparticles was at 271°C that was followed by another peak at 409.01, as an exothermic peak.[40] As shown in Figure 7B, the DSC thermogram of 5-FU-LMWCH-NPs showed a tiny curved-endothermic peak at 90°C followed by a large endothermic peak at approximately 234°C, corresponding to the melting point of 5-FU (273°C)[41,42] indicating that 5-FU is present in its crystalline form. Tiny third and fourth exothermic peaks were noted at 450°C and 554.17°C, respectively representing decomposition of material i.e carrier dosage system. TGA thermogram characterization was used to establish the pattern of the new modification polymer. Chemically cross-linked LMWCH-co-NPs showed higher thermal stability than non-cross-linked NPs. TGA peaks represented mass loss at 100.29°C was 11.78%, at peak 245.43°C was 19.21%, at 280.27°C was 37.59%, at 525.60°C was 51.86% and at 579.68°C was 75.40%, respectively which indicated disintegration that undoubtedly reduction of endothermic peaks in height and sharpness due to thermal stability of low molecular weight cross linked chitosan (LMWCH-NPs) as shown in Figure 7C.[43] TGA thermogram have been shown from Figures 7D, LMWCH-co-NPs (unloaded), showed decomposition temperatures that were almost same as those of 5-FU as after cross-linking with GA, endothermic peak of LMWCH shifted to 106.09°C TGA peak mass loss was 10.7%; this indicated that
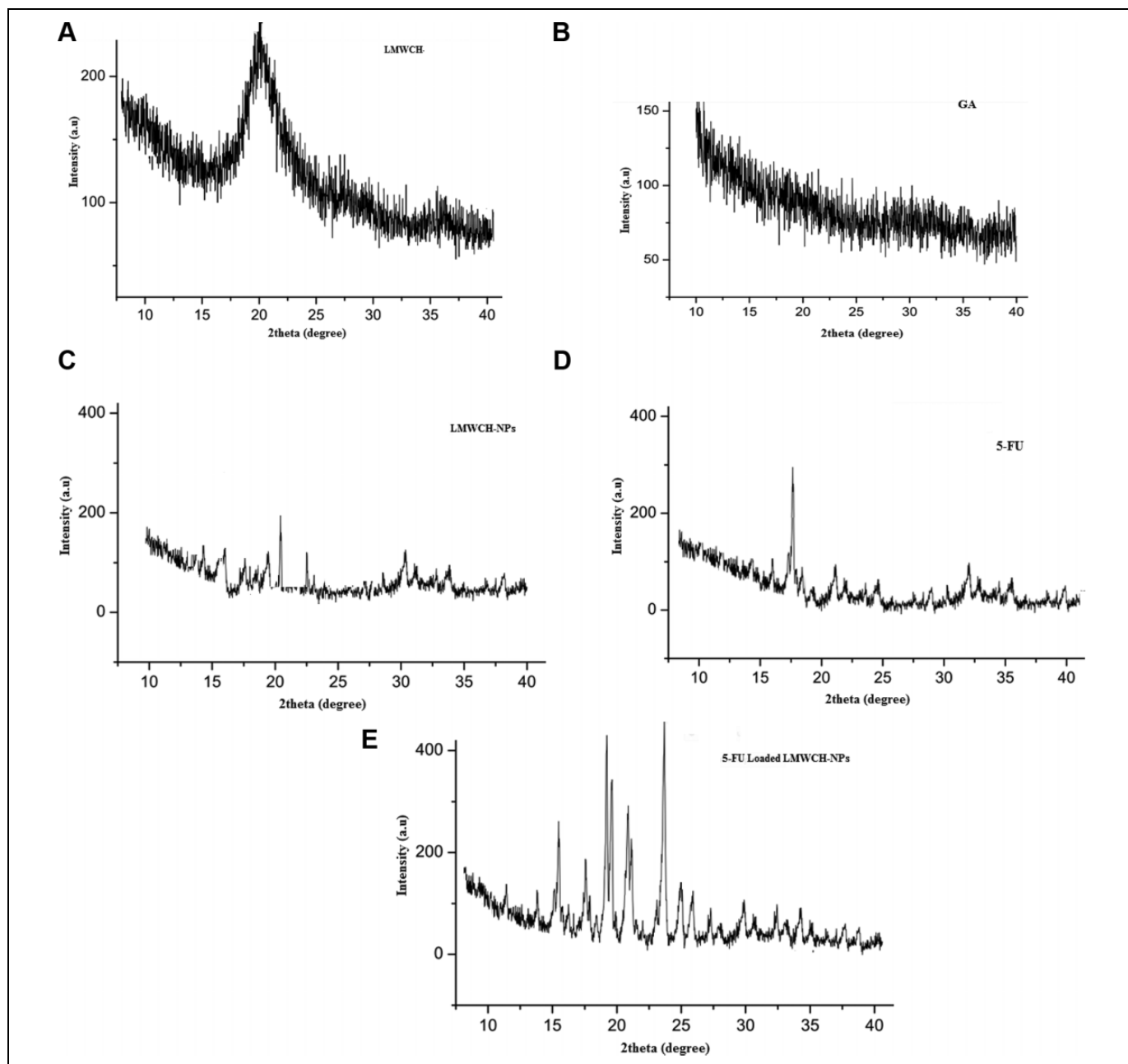
Figure 6. A, PXRD diffractogram of pure LMWCH. B, PXRD diffractogram of glutaraldehyde (GA). C, PXRD diffractogram of LMWCH-NPs. D, PXRD diffractogram of pure 5-FU. E, PXRD diffractogram of 5-FU-LMWCH-NPs.

chemical interaction of LMWCH with GA as well as rigidity of LMWCH matrix at higher temperatures. Subsequent TGA peaks represented mass loss at peak 282.85°C was 18.93% and at 558.95°C was 94.41%, respectively this peak disappeared. The thermogravimetry curve showed that there was no change in the melting point of 5-FU, indicating no chemical interaction between 5-FU and LMWCH-CO-GA-NPs.[44,45] Similar DSC-TGA thermogram results have reported that cross-linked nanoparticles are more rigid and temperature stable than non-cross-linked NPs and transfer endothermic peaks to higher temperatures.[31,46,47]

Drug Release Studies by UV-Vis Spectrophotometer

In the current study, we determined a two-phase set free of 5-FU from LMWCH-co-GA-5-FU NPs with burst release initially followed by controlled release of 5-FU. As shown in Table 4, at the end of this study (i.e., 24 h), 5-FU release was more efficient in alkaline media at high pH 7.4 than in acidic environments at low pH 1.2. An insignificant release of 5-FU was observed at acidic pH of tumors from low molecular weight chitosan nanoparticles (5-FU/GA-co-LMWCH-NPs) as compared to healthy cells. Previous studies have reported
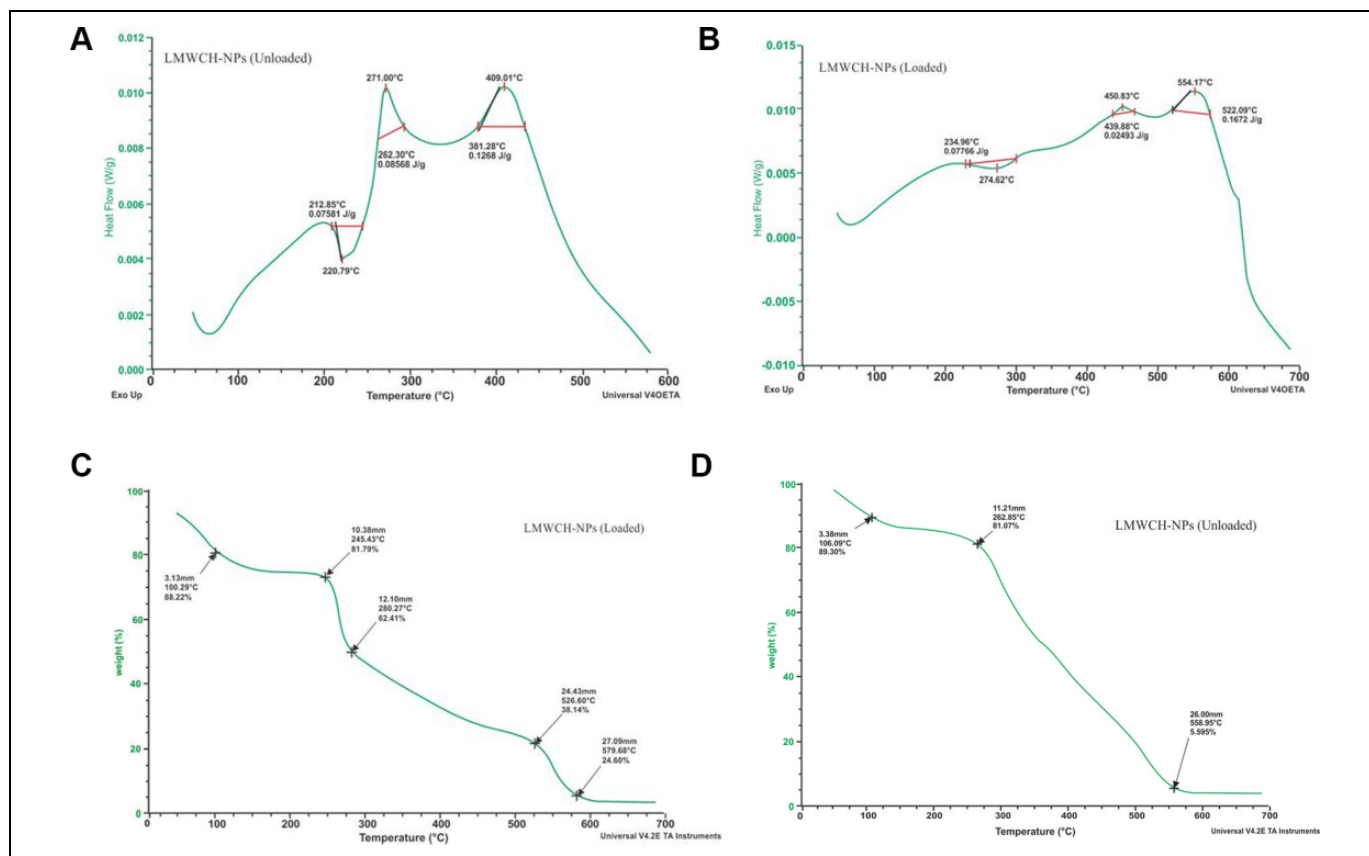
Figure 7. A, DSC thermogram of LMWCH-co-GA-NPs (unloaded). B, DSC thermogram of 5-FU-LMWCH-NPs (Loaded).C, TGA thermogram of LMWCH-NPs (loaded). D, TGA thermogram of GA-co-LMWCH-NPs (unloaded).

Table 4. Effect of % (w/w) Composition of NPs on Mean Values of EE% and Cumulative Drug Release After 24 h Dissolution.

Formulation code	LMWCH: drug %	GA%	EE%	Cumulative drug release (%age)	
				pH 1.2	pH 7.4
5-FU1	2:1	0.1	64.36	32.83	90.39
5-FU2	3:1	0.15	74.28	38.82	97.08
5-FU3	4:1	0.20	88.96	32.78	98.03
5-FU4	5:1	0.25	86.35	37.55	58.87
5-FU5	3:1	0.25	72.55	32.45	55.06
5-FU6	3:1	0.20	60.45	33.56	44.74

that via strong hydrogen bonding between 5-FU and nanoparticles at physiological pH (pH 7.4) and have an efficient release behavior in contrast to acidic conditions, there is the possibility of more H+ ions available to cancel out drug-loaded NP formulations, thus tumbling interactions, significantly improved efficacy in real time and low specificity.[30,45,48-50]

Dissolution Kinetic Analysis

The prepared nanoparticle formulations showed a sustained drug release for at least 16 h, except for 5-FU3, as shown in
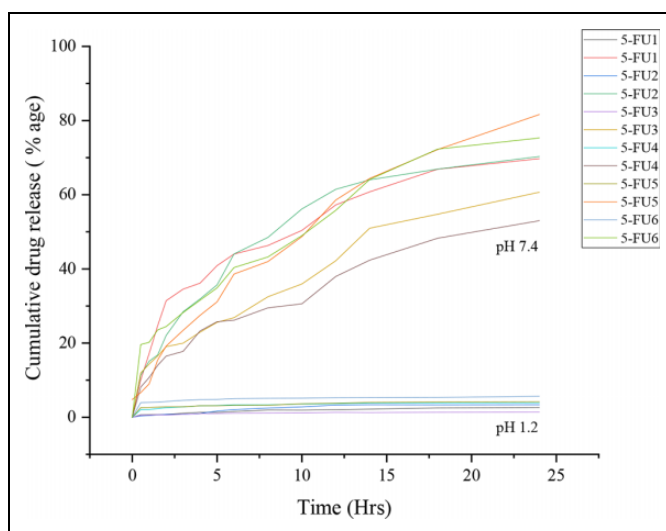

Figure 8. Comparison of 5-FU release of 5-FU-NPs at pH 1.2 and pH 7.4.

Figure 8 and the cumulative %age of drug release (98.3%) increased with an increase in low molecular weight chitosan nanoparticles (LMWCH-NPs). A significant ($P < 00.5$) difference in the rate and extent of drug release was observed in all formulations, with greater than 90% cumulative drug release in

Table 5. Determination of Coefficient (R^2) K & Release Exponent of Various 5-FU Release Kinetic Models.

Sample code	pH	Higuchi		First order		Zero order		Peppas	
		R	$K_2t^{1/2}$	R	K_1tK_1t	R	K_0t	R	N
5-FU1	1.2	0.9357	1.6819	0.6256	1.8217	0.9910	0.8135	0.9935	0.45
	7.4	0.9758	7.9745	0.6483	2.1237	0.9764	9.2156	0.9975	0.65
5-FU2	1.2.	0.9167	7.5181	0.5823	1.7972	0.9845	1.1187	0.9811	0.81
	7.4	0.9857	4.3547	0.6738	2.9452	0.9872	7.5782	0.9939	0.65
5-FU3	1.2	0.9555	0.9185	0.6737	1.9378	0.9853	0.8913	0.9864	0.79
	7.4	0.8345	5.1679	0.6197	1.9143	0.9538	9.2206	0.9914	0.83
5-FU4	1.2	0.9335	1.3122	0.6591	1.4775	0.9784	0.8591	0.9856	0.65
	7.4	0.8993	7.5274	0.6843	2.2751	0.9955	7.9568	0.9829	0.75
5-FU5	1.2.	0.9763	0.8921	0.7123	2.5174	0.9917	0.9345	0.9956	0.71
	7.4	0.9483	6.3957	0.7937	2.1393	0.9943	9.3137	0.9955	0.66
5-FU6	1.2	0.9134	1.7123	0.5967	3.3207	0.9779	1.1162	0.9867	0.77
	7.4	0.9148	8.5587	0.6471	3.1628	0.9862	8.6945	0.9973	0.53

Table 6. Stability Studies of 5-FU/GA-LMWCH-NPs.

	Particle size (nm)		
Months	At room temp.	At 45°C	At 4°C
0	200	200	200
1	200	200	200
2	200	200	200
3	199	199	199
4	199	198	198
5	198	199	199
6	198	198	198

	Drug contents (%)		
Months	At room temp.	At 45°C	At 4°C
0	100	100	100
1	98	98	98
2	97	97	97
3	99	98	99
4	98	98	98
5	99	99	98
6	99	98	98

age of drug.[47,51-53] The nanoparticle formulation 5-FU1 contained the lowest amount of cross-linker and the highest amount of loaded 5-FU. As shown in Table 5, drug release was evaluated by application of the zero-order, first-order, Higuchi, Korsmayer-Peppas, and Peppas models indicated that the 5-FU release pattern from the prepared NP formulations was best fitted to the kinetic model with R^2 values close to 1.[49,50,54]

Stability Studies

It was performed on the best LMWCH-co-GA-NPs formulation (5-FU3) only in terms of particle size and drug content, and no significant variations were observed before and after stability studies. The data of "0" day and 6 month was subjected to "t" test and result was insignificant ($P < 0.05$) which showing stability of synthesized nanoparticles formulations[52,55] at both room temperature and refrigerator as it was found to be in Table 6.

Statistical Analysis

A significant ($P < 00.5$) difference in the rate and extent of drug release was observed in all 5-FU/GA-co-LMWCH-NP formulations was greater than 90%.

24 h. This may be due to an increase in low molecular weight chitosan polymer density or matrix and diffusion path length that the drug has to transverse. 5-Flourouracil release was characterized by a burst release followed by a moderate, slow release. The biphasic pattern of drug release is characteristic of diffusion kinetic matrix diffusion kinetics. By increasing the polymer concentration, burst release can be condensed, resulting in sufficient encapsulation efficiency (EE %) and shrinking the surface area associated with the drug. The concentration of the cross-linking agent, glutaraldehyde (GA), significantly reduced the rate and extent of drug release ($P > 0.05$). Our optimized nanoparticle formulation 5-FU3 had the maximum amount of cross-linker glutaraldehyde; thus, (5-FU3) trapped the least amount of 5-FU and in phosphate buffer pH 7.4 at 37°C, showing rapid release %

Conclusions

We have developed 5-FU/GA-co-LMWCH-NPs for the purpose of delivering 5-FU in a sustained manner for 12-24 h, and we modified them for control and slow release by cautiously adjusting the composition of NPs. 5-FU is a hydrophilic acidic drug with low entrapment efficiency (EE %) in NPs. FTIR observations showed that interactions between 5-FU and LMWCH were absent. The DSC/TGA and PXRD curves confirmed the thermal stability of the NPs. Drug release was found to be diffusion-controlled at 39°C and model-dependent kinetics (n < 0.5), which drastically delayed water absorption without any chemical modification. Hence, targeted specified

platforms with enhanced bioavailability and cost-effective biomaterials for oral controlled drug delivery (OCDDS).

Declaration of Conflicting Interests

The author(s) declared no potential conflicts of interest with respect to the research, authorship, and/or publication of this article.

ORCID iD

Aisha Sethi https://orcid.org/0000-0002-7963-5599

References

1. Global Cancer Statisctics. Published 2020. https://acsjournals.onlinelibrary.wiley.com.dio/full/10.3322/caac.21660
2. Siegel RL, Miller KD, Jemal A. Cancer statistics. *CA Cancer J Clin*. 2020;68(1):7-30. doi:10.3322/caac.21442
3. Xu X, Ho W, Zhang X, Bertrand N, Farokhzad O. Cancer nanomedicine: from targeted delivery to combination therapy. *Trends Mol Med*. 2015;21(4):223-232. doi:10.1016/j.molmed.2015.01.001
4. Bamrungsap S, Zhao Z, Chen T, et al. Nanotechnology in therapeutics: a focus on nanoparticles as a drug delivery system. *Nanomedicine (Lond)*. 2012;7(8):1253-1271. doi:10.2217/nnm.12.87
5. Acharya S, Sahoo SK. PLGA nanoparticles containing various anticancer agents and tumour delivery by EPR effect. *Adv Drug Deliv Rev*. 2011;63(3):170-183. doi:10.1016/j.addr.2010.10.008
6. Mohammed MA, Syeda JTM, Wasan KM, Wasan EK. An overview of chitosan nanoparticles and its application in non-parenteral drug delivery. *Pharmaceutics*. 2017;9(4):53. doi:10.3390/pharmaceutics9040053
7. Moghimi SM, Hunter AC, Murray JC. Long-circulating and target-specific nanoparticles: theory to practice. *Pharmacol Rev*. 2001;53(2):283-318.
8. Kumari A, Yadav SK, Yadav SC. Biodegradable polymeric nanoparticles based drug delivery systems. *Colloids Surf B Biointerfaces*. 2010;75(1):1-18. doi:10.1016/j.colsurfb.2009.09.001
9. Zheng T, Liang Y, Ye S, He Z. Superabsorbent nanoparticles as carriers for the controlled-release of urea: experiments and a mathematical model describing the release rate. *Biosys Eng*. 2009;10(2):44-50.
10. Qi L, Xu Z, Jiang X, Hu C, Zou X. Preparation and antibacterial activity of chitosan nanoparticles. *Carbohydr Res*. 2004;339(16):2693-2700. doi:10.1016/j.carres.2004.09.007
11. Silva GA, Coutinho OP, Mano JF, Reis RL. Preparation and characterisation in simulated body conditions of glutaraldehyde crosslinked chitosan membranes. *J Mater Sci Mater Med*. 2005;15(10):1105-1112.
12. Peppas NA, Bures P, Leobandung W, Ichikawa H. Hydrogels in pharmaceutical formulations. *Eur J Pharm Biopharm*. 2000;50(1):27-46.
13. Qiu Y, Park K. Environment-sensitive nanoparticles for drug delivery. *Adv Drug Deliv Rev*. 2001;53(4):321-339.
14. Lin CC, Metters AT. Hydrogels in controlled release formulations: network design and mathematical modeling. *Adv Drug Deliv Rev*. 2006;58(12-13):1379-1408.
15. Geever LM, Cooney CC, Lyons JG, et al. Characterisation and controlled drug release from novel drug-loaded nanoparticles. *Eur J Pharm Biopharm*. 2008;6(9):1147-1159.
16. Kim JO, Kabanov AV, Bronich TK. Polymer micelles with cross-linked polyanion core for delivery of a cationic drug doxorubicin. *J Control Release*. 2009;138(3):197-204.
17. Censi R, Di Martino P, Vermonden T, Hennink WE. Nanoparticles for protein delivery in tissue engineering. *J Control Release*. 2012;16(1):680-692.
18. Unsoy G, Khodahollah R, Yalcin S, Mutlu P, Gunduz U. Synthesis of doxorubin loaded magnetic chitosan nanoparticles. *J Biotechnol*. 2014;1(4):10-21.
19. Haznedar S, Dortunc B. Preparation and in vitro evaluation of Eudragit microspheres containing acetazolamide. *Int J Pharm*. 2004;26(9):131-140.
20. Verheyen E, van der Wal S, Deschout H, et al. Protein macromonomers containing reduction-sensitive linkers for covalent immobilization and glutathione triggered release from dextran nanoparticles. *J Control Rel*. 2011;15(6):329-336.
21. Peracchia MT, Fattal E, Desmaële D, et al. Stealth (®) PEGylated polycyanoacrylate 113 nanoparticles for intravenous administration and splenic targeting. *J Controlled Release*. 1999;60:121-128.
22. Naik K, Chatterjee A, Prakash H, Kowshik M. Mesoporous TiO_2 nanoparticles containing Ag ion with excellent antimicrobial activity at remarkable low silver concentrations. *J Biomed Nanotechnol*. 2013;9(4):664-673.
23. Midgley R. *Systemic Adjuvant Therapy of Colon Cancer*. Taylor & Francis; 2002:5063-5069.
24. Wang ZL. Transmission electron microscopy of shape-controlled nanocrystals and their assemblies. *J Phy Chem B*. 2000;10(4):1153-1175.
25. Sakamoto J, Oba K, Matsui T, Kobayashi M.Efficacy of oral anticancer agents for colorectal cancer. *Dis Colon Rectum*. 2006;4(9):82-91.
26. Diasio RB, Harris BE. Clinical pharmacology of 5-fluorouracil. *Clin Pharma*. 1989;16(4):215-237.
27. Szepes A, Makai Z, Blumer C, Mader K, Kasaa P Jr, Szabo-Revasz P. Characterization and drug delivery behaviour of starch-based nanoparticles prepared via isostatic ultrahigh pressure. *Carbohydrate Poly*. 2008;72:571-578.
28. Patel MN, Lakkadwala S, Majrad MS, et al. Characterization and evaluation of 5-fluorouracil-loaded solid lipid nanoparticles prepared via a temperature-modulated solidification technique. *AAPS Pharm Sci Tech*. 2014;15:1498-1508.
29. Costa MM, Terezo AJ, Matos AL, Moura WA, Giacometti JA, Sombra ASB. Impedance spectroscopy study of dehydrated chitosan and chitosan containing LiClO4. *Physica B Condens Matter*. 2010;405(21):4439-4444.

30. Pawlak A, Mucha M. Thermogravimetric and FTIR studies of chitosan blends. *Thermochimica Acta*. 2003;396(1):153-166.

31. Fournier E, Passirani C, Colin N, Bretona P, Sagodiraa S, Benoitb JP. Development of novel 5-FU-loaded poly (methylidene malonate2.1.2)-based microspheres for the treatment of brain cancers. *Eur J Pharm Biopharm*. 2004;57:189-197.

32. Olukman M, Şanlı O, Solak EK. Release of anticancer drug 5-fluorouracil from different ionically crosslinked alginate beads. *J Biomat Nanobiotechnol*. 2012;3:469-479.

33. Morales-Sánchez A, Barreto J, Domínguez C, et al. DC and AC electroluminescence in silicon nanoparticles embedded in silicon-rich oxide films. *Nanotechnol*. 2010;21(8):57-80.

34. Lu C, Wu N, Jiao X, Luo C, Cao W. Micropatterns constructed from Au nanoparticles. *Chem Commun*. 2003;1(9):1056-1057.

35. Zhang DY, Shen XZ, Wang JY, Dong L, Zheng YL, Wu LL. Preparation of chitosan-polyaspartic acid-5-fluorouracil nanoparticles and its anti-carcinoma effect on tumor growth in nude mice. *World J Gastroenterol*. 2008;14(4): 3554-3562.

36. Mitra S, Gaur U, Ghosh PC, Maitra AN. Tumour targeted delivery of encapsulated dextran-doxorubicin conjugate using chitosan nanoparticles as carrier. *J Control Release*. 2001;74:317.

37. Ziyaur R, Kanchan K, Roop K, Mushir A, Naseem AC, Areeg AAS. Characterization of 5-flurouracil microspheres for colonic delivery. *AAPS Pharm Sci Tech*. 2006;7(2):E47.

38. Boisdron-Celle M, Menei P, Benoit JP. Preparation and characterization of 5-fluorouracil-loaded microparticles as biodegradable anticancer drug carriers. *J Pharm Pharmacol*. 1995;47: 108-114.

39. Lin YS, Ming LJ, Peng J, Fu YK, Lee S. Radical annihilation of c-ray-irradiated contact lens blanks made of a 2-hydroxyethyl methacrylate copolymer at elevated temperatures. *J Appl Polymer Sci*. 2010;11(7):3114-3120.

40. Lai LF, Guo HX. Preparation of new 5-fluorouracil-loaded zein nanoparticles for liver targeting. *Int J Pharm*. 2011;404(2): 317-323.

41. Hans ML, Lowman AM. Biodegradable nanoparticles for drug delivery and targeting. *Curr Opinion Solid St M*. 2010;6(6): 319-327.

42. Chiu LK, Chiu WJ, Cheng YL. Effects of polymer degradation on drug release—a mechanistic study of morphology and transport properties in 50:50 poly (DL-lactide-co glycolide). *Int J Pharm*. 1995;12(6):169-178.

43. Li P, Wang Y, Peng Z, She MF, Kong L. Physichemical property and morphology of 5-fluorouracil loaded chitosan nanoparticles.

In: *International Conference on Nanoscience Nanotechnology (ICONN)*, Sydney, NSW, Australia, February 22-26, 2010, pp. 248-250. Sydney: IEEE.

44. Hambrecht A, Yamamoto H, Takeuchi H, Kawashima Y. Observation in simultaneous microencapsulation of 5-fluorouracil and leucovorin for combined pH-dependent release. *Eur J Pharm Biopharm*. 2005;59:367-371.

45. Rao K, Rao KM, Kumar PN, Chung ID. Novel chitosan-based pH sensitive micro-networks for the controlled release of 5-fluorouracil. *Iran Polymer J*. 2010;19:265-276.

46. Machover D. A comprehensive review of 5-fluorouracil and leucovorin in patients with metastatic colorectal carcinoma. *Cancer*. 1997;80:1179-1187.

47. Satta F, Franchi F. Beyond 5-fluorouracil monochemotherapy in colorectal cancer—it is time. *J Chemother*. 1997;9:431-435.

48. Khan MI, Madni A, Ahmad S, Mahmood MA, Rehman M, Ashfaq M. Formulation design and characterization of a non-ionic surfactant based vesicular system for the sustained delivery of a new chondroprotective agent. *Brazil J Pharmaceuti Sci*. 2015;51:607-615.

49. Khan MI, Madni A, Peltonen L. Development and in-vitro characterization of sorbitan monolaurate and poloxamer 184 based niosomes for oral delivery of diacerein. *Eur J Pharma Sci*. 2016;95:88-95.

50. Kim YH, Shin SW, Kim BS, et al. Paclitaxel, 5-fluorouracil, and cisplatin combination chemotherapy for the treatment of advanced gastric carcinoma. *Cancer*. 1999;85:295-301.

51. Ramesh Babu V, Sairam M, Hosamani KM, Aminabhavi TM. Development of 5-fluorouracil loaded poly (acrylamide-co-methylmethacrylate) novel core-shell microspheres: in vitro release studies. *Int J Pharma*. 2006;325:55-62.

52. Lamprecht A, Yamamoto H, Takeuchi H, Kawashima Y. Microsphere design for the colonic delivery of 5-fluorouracil. *J Control Rel*. 2003;90:313-322.

53. Paul D, Robeson LM. Polymer nanotechnology: nanocomposites. *Polymer*. 2008;49:3187-3204.

54. Dash S, Murthy PN, Nath L, Chowdhury P. Kinetic modeling on drug release from controlled drug delivery system. *Acta Pol Pharm*. 2010;67(3):217-223.

55. The European Agency for the evaluation of medicinal products. Stability testing guidelines: stability testing of new drug substances and products. ICH-Technical Coordination, EMEA. Published 2003. Accessed February 20, 2003. [21 screens]. http://www.emea.eu.int